Stability analysis and robust damping of multiresonances in distributed-generation-based islanded microgrids

Saim, Abdelhakim; Houari, Azeddine; Guerrero, Josep M.; Djerioui, Ali; Machmoum, Mohamed; Ahmed, Mourad Ait

Published in:
IEEE Transactions on Industrial Electronics

DOI (link to publication from Publisher):
10.1109/TIE.2019.2898611

Publication date:
2019

Document Version
Accepted author manuscript, peer reviewed version

Stability Analysis and Robust Damping of Multi-Resonances in Distributed Generation based Islanded Microgrids

Abdelhakim Saim, Azeddine Houari, Josep M. Guerrero, *Fellow, IEEE,* Ali Djerioui, Mohamed Machmoum, and Mourad Aït Ahmed

***Abstract*— This paper develops useful tools to address resonance phenomena in islanded microgrids (MGs). The modeling of islanded MGs is first proposed based on simplified passive circuits where both Thevenin's and Norton's equivalent representations are considered to describe the dynamic of the interconnected distributed generators (DGs) and loads. It is shown that the interactions between the interconnecting passive filters as well as the presence of disturbing loads leads to complex resonance phenomena at various frequencies, which reduces power quality and even leads to instability. To cope with these issues, an active damping method based on a robust disturbances observer is proposed. The proposed method is designed to mitigate resonance issues encountered in islanded MGs with multiple electronically interfaced DGs and loads. This damping method is seamlessly incorporated into the conventional hierarchical control structure through the direct control signal modification. The main merit of the proposed approach is to calculate the appropriate resonances compensating signal without prior knowledge of the system parameters and without affecting the control bandwidth. Simulation and experimental results are provided to show the effectiveness of the developed damping approach.**

***Index Terms*—Active damping, islanded microgrid, multi-resonance, robust observer,**

I. INTRODUCTION

THE progress realized in recent years in power electronics and the advent of new cutting-edge technologies make the integration of renewable energy sources and energy storage systems very attractive [1]. Moreover, the development of these technologies offers solutions to extend the electric coverage to isolated places with the deployment of small to medium scale microgrids (MGs) with multiple electronically interfaced distributed generators (DGs) [2].

These systems can operate close to end-users with either grid-connected or islanded mode, which improves local grid reliability and resilience, increases energy efficiency and brings additional benefits regarding investment reduction for future grid reinforcement and expansion [3]. Besides, these grid configurations should be able to locally solve energy problems and secure safe and stable operations especially in islanded mode wherein an effective control strategy must be applied [4]. The control of DG based MGs usually adopts a hierarchical control structure with primary, secondary and tertiary control levels [5]-[6]. The resulting control scheme achieves satisfactory performances, but remains faced to major issues related to the presence of interconnecting passive filters with inherent resonance phenomena, which ineluctably reduce power quality and weaken their global stability [7]. Indeed, DGs are typically interfaced to a point of common coupling (PCC) through LC, and LCL passive harmonic filters, which provides sufficient switching harmonic attenuation, but brings resonances at various frequencies [8]. Moreover, the presence of passive elements including passive filters, inductive line impedances, parasitic shunt capacitors and household capacitive-inductive loads with trivial dissipative elements brings complex resonance interactions in the MG [9].

The induced resonance phenomena affect both transient and steady-state control performances and even lead to severe stability issues [10]. In addition, the stability and power quality of islanded MGs get worse with the proliferation of nonlinear and disturbing loads. Indeed, the presence of disturbing loads with either constant voltage or constant power characteristics brings additional resonance interactions [11].

In order to overcome the aforementioned concerns, the use of well-designed control procedures is required. In this context, various control techniques are proposed in order to relieve MGs performances, maintain suitable voltage waveforms, and reduce the amount of circulating currents through an accurate power sharing control [12]. Among the

Manuscript received July 20, 2018; revised November 09, 2018 and January 09, 2019; accepted January 21, 2019.

A.Saim is with the Department of Control and Instrumentation, University of Sciences and Technology Houari Boumediene, 16111 Algiers, Algeria (e-mail: asaim@usthb.dz).

A. Houari is with the Institut de Recherche en Energie Electrique de Nantes Atlantique, University of Nantes, 44602 Saint-Nazaire, France (e-mail:azeddine.houari@univ-nantes.fr).

J.M. Guerrero is with the Department of Energy Technology, Aalborg University, 9220 Aalborg, Denmark (e-mail:joz@et.aau.dk).

A. Djerioui is with the Department of Electronics, M'Sila University, 28000 M'Sila, Algeria (e-mail: ali.djerioui@etu.univ-nantes.fr).

M. Machmoum, M. Aït-Ahmed, are with the Institut de Recherche en Energie Electrique de Nantes Atlantique, University of Nantes, 44602 Saint-Nazaire, France (e-mail:mohamed.machmoum@univ-nantes.fr ; ait-ahmed-m@univ-nantes.fr).

proposed power control schemes, wireless power sharing controllers have attracted the attention of many researchers with a focus on droop schemes [13]. Indeed, droop based controllers have seen a considerable growth and substantial modifications have been proposed in addition to the association of various virtual output impedances [14]. The addition of virtual passive elements aims to enforce the output impedance behavior of each DG unit, handle the existing line impedance unbalance, improve power sharing accuracy between the parallel-connected DG systems and provide further resonance damping capability through virtual resistors [15]. In addition, to maintain the whole system stability and properly dampen its potential unstable dynamic, numerous strategies have been proposed in the literature using either, passive or active damping solutions [16]. The use of passive damping solutions consists on the addition of supplementary passive elements with energy dissipative characteristics to dampen out the undesired resonances [17]. This method presents effective damping performances, but brings additional power losses and downgrades the harmonic attenuation performances of the system for high frequencies limiting it applicability to low power systems. Alternatively, the use of active damping solutions with either filter-based or feedback-based control methods is preferred due to their efficiency and flexibility against system adaptation and expansion [18]. These methods show great promise for resonance mitigation, but involve the use of additional measurements and complementary control loops. For instance, the feedback-based damping methods involve additional state feedbacks with either capacitor current [19], inductor current [20], or capacitor voltage feedbacks [21]. The use of additional state feedback ensures wider damping regions, but at the expense of the control complexity and cost. On the other hand, the filter based damping approaches incorporate additional filters to the control loops with the aim to suppress the undesired dynamic in closed loop and improve system stability margins around the resonance frequency using mainly Notch, Lead-Lag Network and Biquad filers [22]–[25]. The filter-based methods remain sensitive to parameters uncertainties and still rely on an accurate resonance frequency estimate [26]. Indeed, the design of the filter-based methods is based on the physical characteristics of the system, which let them ineffective in weak grids given that the output impedance may vary in a wide range [27]. Moreover, the introduction of additional filters may reduce the dynamic of the control system and its efficacy for disturbance rejection. Although meaningful improvements are found in the literature for both filter based and feedback based damping methods, their performances are still dependent either on an accurate resonance frequency estimation or on a comprehensive system modeling. Moreover, these contributions focus only on grid-connected DGs with single resonance frequencies without addressing issues encountered in systems with multi resonance frequencies. The resonance characteristic of grid-connected MGs with multiple DG systems is analyzed in [28], revealing the existence of complex resonance interactions leading to multi resonance frequencies. It is shown that these resonances are dependent on the number, type and composition ratio of the paralleled DG units. This relationship is further reinforced in islanded MGs where critical interactions can occur between upstream DG units and downstream loads [29]. At this level, supplementary research efforts are needed to investigate for resonance damping and stability enhancement in DG based islanded MGs aiming at securing safe and stable operations.

This paper provides useful tools to investigate and fix resonance phenomena encountered in islanded MGs with multiple electronically interfaced DGs and loads. Indeed, a comprehensive MG modeling is first proposed based on simplified passive circuits where both Thevenin's and Norton's equivalent representations are considered to describe the dynamic behavior of the interconnected DGs and loads. The proposed model reveals that the resonance characteristic of islanded MGs presents a frequency-varying behavior resulting in complex resonances at multiple harmonic and sub-harmonic frequencies. After that, an active damping method is proposed based on a robust disturbance observer to dampen out these resonances and enhance the stability of islanded MGs. The proposed method is based on the reconstruction of the disturbing nonlinearities using a robust nonlinear observer with the merit to timely estimate and compensate for resonance disturbances. The use of a nonlinear observer is motivated by the particular context of islanded MGs where an accurate reconstruction of the resonance disturbances that appear at multiple and time-varying frequencies is crucial to achieve a targeted resonance damping. Indeed, compared to the existing methods, the globally convergent estimator presents several advantages for periodic signal estimations with a powerful ability to accommodate for time-varying disturbances [30]. Indeed, this observer is conceptually dedicated for sinusoidal signal estimation given that the signal model is implicitly immersed in the observer. From the structural point of view, this observer is inherently stable, highly selective and robust to signal state and frequency variations since it presents a nonlinear characteristic with an integral chain that achieves a robust stabilization and disturbance rejection [31]. Moreover, the structural property of this observer offers additional degrees of freedom with intermediate setting parameters to shape the desired response performances, namely settling the speed of convergence and precision, which is essential in practical implementations.

More specifically, the main merits of the proposed damping method rely on it:

1- Robustness to resonance frequency variations even in the presence of multiple resonance peaks. Indeed, the proposed method is robust to system and load parameters variations, and accordingly to resonance frequencies variation since it is synthetized based on a robust observer that is able to reconstruct the undesired resonance disturbances without prior knowledge of system parameters and frequencies. This fact is particularly important in islanded MGs wherein the equivalent impedance varies depending on the connected DGs and loads, which moves resonances within a wide frequency range resulting in challenging resonance characteristics with multiple and frequency varying resonance peaks.

This article has been accepted for publication in a future issue of this journal, but has not been fully edited. Content may change prior to final publication. Citation information: DOI 10.1109/TIE.2019.2898611, IEEE Transactions on Industrial Electronics

2- High dynamic to not affect controllers' bandwidth. Indeed, the bandwidth of the proposed damping method is sufficiently higher that of the inner controllers, which guarantee relevant performances for both transient and steady state. In this way, the control dynamic remains almost unchanged and harmonic filtering performances are not compromised since that the proposed method acts only around the undesired resonance frequencies.
3- Simple implementation with limited computational time and no extra measurements. The proposed damping method is implemented through an additional control loop that is seamlessly incorporated to the conventional hierarchical control scheme using only the capacitor voltage measure, which avoid any additional materials or measurements.

Simulation and experiment results are provided to show the effectiveness of the developed damping approach.

II. MODELING OF ISLANDED MICROGRIDS

This section focuses on the development of a comprehensive modeling of islanded MGs. As shown in Fig.1, the configuration of MGs allows supplying various load circuits through the integration of multiple DG units.

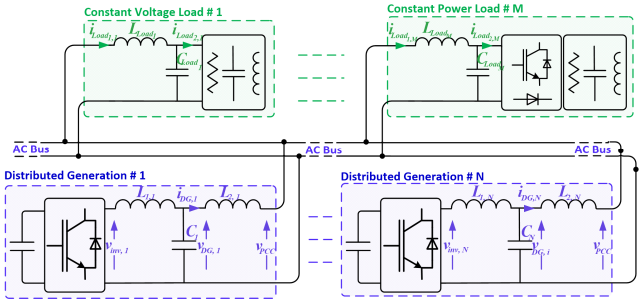

Fig. 1. Circuit representation of an islanded MG

A. Distributed generators modeling

As illustrated in Fig.1, DGs under study consist of tightly controlled single-phase inverters with output LC-L filtering stages. Indeed, LC-L filters are employed to connect DG inverters to a point of common coupling (PCC) and filter out the resulting switching harmonics. Note that, line inductances are lumped together with the LC-L filters, while the illustrated DC-links are assumed as constant voltage sources.

Therefore, each DG unit can be modeled based on the dynamic behavior of it corresponding output LC-L filter and can be directly obtained by applying the voltage divider theorem as follows:

$$v_{PCC} = \frac{Z_{c,i}}{Z_{c,i} + Z_{L_{1,i}}} v_{inv,i} - \left(\frac{Z_{c,i} Z_{L_{1,i}}}{Z_{c,i} + Z_{L_{1,i}}} + Z_{L_{2,i}} \right) i_{DG,i} \qquad (1)$$

where, $v_{inv,i}$ and v_{PCC} represent the inverter voltage and the PCC voltage, respectively, while the output current of the i^{th} DG unit is given by $i_{DG,i}$. As can be noted, an impedance based approach with $Z_{L_{1,i}} = L_{1,i}s$, $Z_{c,i} = 1/C_i s$ and $Z_{L_{2,i}} = L_{2,i}s$ was preferred in order to ease the equation handling. $L_{1,i}$ and $L_{2,i}$ denote the inverter-side and the line-side filter inductances, respectively, while C_i represents the filter capacitance. Note that all equivalent series resistors are neglected in order to emulate a critical case where no dissipative elements exist.

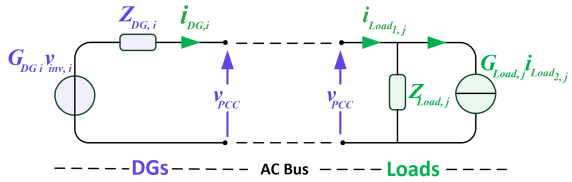

Fig. 2. Equivalent circuits of DGs and Loads

Obviously, (1) corresponds to a Thevenin circuit including an ideal voltage source $G_{DG,i} v_{inv,i}$ and an output equivalent impedance $Z_{DG,i} = Z_{c,i} \parallel Z_{L_{1,i}} + Z_{L_{2,i}}$.

$$v_{PCC} = G_{DG,i} v_{inv,i} - Z_{DG,i} i_{DG,i} \qquad (2)$$

B. Load modeling

Fig.1 illustrates two main load configurations found in MGs including constant voltage (CVL) and constant power (CPL) loads. A widespread use of these types of loads in both embedded and stationary MGs is expected due to their advantages in terms of operation and flexibility [32]. These load circuits are mainly composed of an LC circuit representing the sub-feeder line impedance coupled to a shunt capacitor along with an electronically interfaced output load. Those loads can be modeled as follows:

$$i_{Load_{1,j}} = \frac{Z_{C_{Load,j}}}{Z_{C_{Load,j}} + Z_{L_{Load,j}}} i_{Load_{2,j}} + \frac{1}{Z_{C_{Load,j}} + Z_{L_{Load,j}}} v_{PCC} \qquad (3)$$

where, $Z_{L_{Load,j}} = L_{Load,j}s$ and $Z_{C_{Load,j}} = 1/C_{Load,j}s$, being $L_{Load,j}$ and $C_{Load,j}$ the load sub-feeder line inductance and shunt capacitance, respectively. $i_{Load_{2,j}}$ represents the load current, and $i_{Load_{1,j}}$ the load filter current. The argument "j" refers to loads connected.

The previous equation suggests that loads may be represented by couples of Norton' terminals. As shown in Fig. 2, this representation includes an ideal current source $G_{Load,j} i_{Load_{2,j}}$ with an equivalent admittance $Y_{Load,j} = 1/Z_{Load,j}$ given that $Z_{Load,j} = Z_{C_{Load,j}} + Z_{L_{Load,j}}$.

$$i_{Load_{1,j}} = G_{Load,j} i_{Load_{2,j}} + Y_{Load,j} v_{PCC} \qquad (4)$$

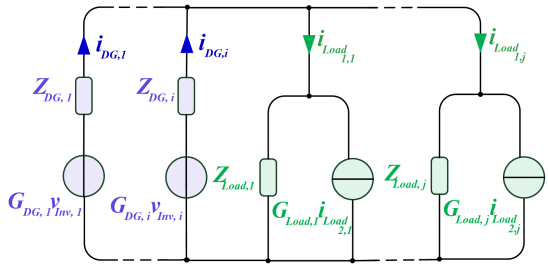

Fig. 3. Equivalent representation of islanded MGs

C. Equivalent model of islanded microgrids

This section combines the models developed above to establish an equivalent model of islanded MGs with N DGs

This article has been accepted for publication in a future issue of this journal, but has not been fully edited. Content may change prior to final publication. Citation information: DOI 10.1109/TIE.2019.2898611, IEEE Transactions on Industrial Electronics

and M loads. Accordingly, the equivalent representation of islanded MGs shown in Fig.3 is obtained by substituting both DGs and loads with their corresponding Thevenin's and Norton's representations.

Therefore, by assuming that the circulating currents are effectively eliminated, i.e., $\sum_{i=1}^{N} i_{DG,i} = \sum_{j=1}^{M} i_{Load_{1,j}}$, the Millman's theorem is used to derive the following PCC's voltage expression.

$$v_{PCC} = \frac{\sum_{i=1}^{N} \frac{G_{DG,i}}{Z_{DG,i}} v_{inv,i} - \sum_{j=1}^{M} G_{Load,j} i_{Load_{2,j}}}{\sum_{i=1}^{N} \frac{1}{Z_{DG,i}} + \sum_{j=1}^{M} \frac{1}{Z_{Load,j}}} \quad (5)$$

The above expression demonstrates that the load bus voltage is directly affected by the behaviour of the connected DGs and loads, which is pointed out below for a typical MG with two parallel DGs ($N = 2$) and a single load ($M = 1$).

$$v_{PCC} = G_1 v_{inv,1} + G_2 v_{inv,2} - Z_1 i_{Load_{2,1}} \quad (6)$$

With

$$G_1 = \frac{Z_{DG,2} Z_{Load,1} G_{DG,1}}{Z_{DG,1} Z_{Load,1} + Z_{DG,2} Z_{Load,1} + Z_{DG,1} Z_{DG,2}}$$
$$G_2 = \frac{Z_{DG,1} Z_{Load,1} G_{DG,2}}{Z_{DG,1} Z_{Load,1} + Z_{DG,2} Z_{Load,1} + Z_{DG,1} Z_{DG,2}} \quad (7)$$
$$Z_1 = \frac{Z_{DG,1} Z_{DG,2} Z_{Load,1} G_{Load,1}}{Z_{DG,1} Z_{Load,1} + Z_{DG,2} Z_{Load,1} + Z_{DG,1} Z_{DG,2}}$$

where, G_1 and G_2 represent DGs side voltage gains expressions associated to the 1st and 2nd DG units, while Z_1 represents the load side impedance expression, respectively. These expressions highlight the complex coupling that exists between DGs and loads, which can lead to strong resonance interactions propagating in the whole MG.

III. Resonance Investigation in Islanded Microgrids

Islanded MGs are subject to critical interactions inducing the proliferation of resonance phenomena, which result in small to large voltage oscillations that affect their performances and even leads to instability. Indeed, these grid configurations face the presence of multiple sources of instability, including LC-L filter resonances and load disturbances, which results in challenging resonance characteristics with multiple frequency-varying resonances. Moreover, these MGs can experience multiple resonances at various harmonic and sub-harmonic frequencies due to the existing hardware unbalances. Indeed, in an islanded MG with N parallel DGs and M loads, the PCC's voltage may experience at least $N + M$ resonances reducing both power quality and system stability. In this section, the developed model is employed to investigate for resonance interactions and propagation in a typical islanded MG composed of two identical DG units and one disturbing Load. The system parameters are listed in Table 1. The parameters used for DG #2 are similar to those of DG #1, which result in the same voltage gain and impedance expressions. The frequency responses of the corresponding DG-side voltage gains $(G_i = v_{pcc}/v_{inv,i},\ i = 1,2)$ and load-side impedances $(Z_i = v_{pcc}/i_{Load_{2,i}},\ i = 1,2)$ expressions, illustrated in Fig. 4 and 5, reveal the presence of a double resonance peak with 50 dB of magnitude at the characteristic resonance frequency of DG #1 and similarly of DG #2 (876 Hz). The disturbing load induces resonance at 263 Hz with more than 100 dB of magnitude while an additional peak appears at 951 Hz due to resonance interactions. In addition, these figures reveal that the presence of undamped resonances exposes similarly the overall MG to instabilities. These figures demonstrate the frequency-varying characteristic of resonances in islanded MGs that move from their respective characteristic resonance frequencies to different resonance frequencies. Moreover, it is shown that the resonance interactions in islanded MGs result in additional resonances at higher frequencies, which let them prone to be exited in presence of transient and steady-state background harmonics resulting in harmonic amplifications. Therefore, the control of islanded MGs should include an effective resonance damping method aimed at limiting resonance propagation and amplification.

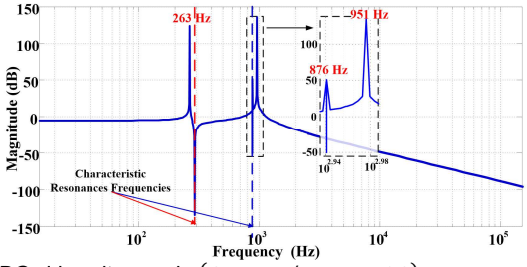

Fig. 4. DG side voltage gain $(G_i = v_{pcc}/v_{inv,i}, i = 1,2)$

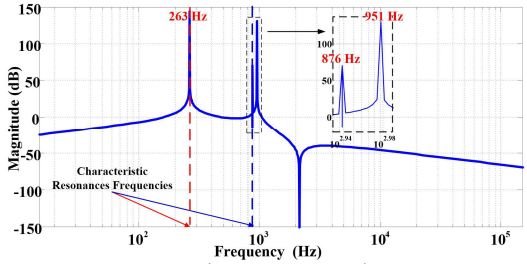

Fig. 5. Load side impedance $(Z_1 = v_{pcc}/i_{Load_{2,1}})$

IV. Resonance Damping in Islanded Microgrids

This section proposes an efficient damping method that benefits from the merits of a robust disturbance observer to reconstruct and compensate for resonances disturbances.

A. Proposed active damping method

The proposed damping method aims to overcome issues related to resonance phenomena in islanded MGs and dampen out resulting harmonic and sub-harmonic disturbances. Indeed, it allows compensating for disturbances through an additional control loop that is seamlessly incorporated to the conventional hierarchical control to shape the control signal of each DG unit according to the undesired voltage harmonic components. For this aim, a robust disturbance observer is employed to reconstruct the introduced disturbances based only on an accurate voltage state and frequency estimation. Indeed, the proposed damping method exploits results of global convergence estimators for measurable periodic signals with unknown amplitudes and frequencies to estimate the fundamental voltage component and block out the undesired voltage harmonic components without affecting the control

This article has been accepted for publication in a future issue of this journal, but has not been fully edited. Content may change prior to final publication. Citation information: DOI 10.1109/TIE.2019.2898611, IEEE Transactions on Industrial Electronics

dynamic of the inner control levels. This method allows estimating the undesired voltage harmonic components without prior knowledge of system parameters and frequencies. Moreover, the control dynamic remains almost unchanged and harmonic filtering performances are not compromised. The block diagram of the proposed damping method given below is illustrated in Fig. 6.

$$v_{inv,i}^{*} = v_{inv,i} - k_d\left(v_{DG,i} - \hat{v}_{DG,i}\right) \quad (8)$$

where, $v_{inv,i}^{*}$ represents the resulting inverter control voltage, while $v_{DG,i}$ represents the measured filter capacitor voltage and $\hat{v}_{DG,i}$ represents the estimation of its fundamental component. k_d is the damping coefficient that is introduced in order to scale the damping ratio.

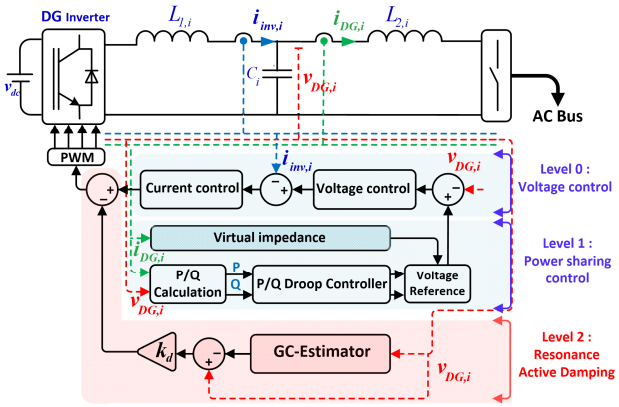

Fig.6. Proposed DGs control strategy with resonance active damping

B. Robust disturbance observer

As pointed out in [31], the problem of sinusoid signal states and frequencies estimation is a well-known problem in system theory where several approaches are proposed to ensure the online estimation of measurable signals. Among these approaches, a globally convergent estimator is proposed in [32] with the ability to track periodic signals with time varying frequencies and amplitudes. Indeed, the underlined globally convergent estimator presents numerous advantages being frequency-independent and robust against amplitude uncertainties even in presence of distorted sinusoid signals with multiple sinusoids of different frequencies. Moreover, this estimator presents satisfactory dynamic with global convergence regardless initial condition and frequency variation, which allows tracking asymptotically sinusoidal signal with proven convergence for many practical applications [33]. Accordingly, it is obvious that this estimator presents interesting features for electric applications, wherein signals are not pure sinusoidal and contain harmonics. In this way, the use of this estimator is preconized to reconstruct the undesired harmonic voltage components based on the fundamental voltage component estimate. Indeed, this estimation method has been exploited for the synthesis of a disturbance observer that acts as a resonance compensator.

Let us consider a sinusoidal signal of the form,

$$y(t) = E_{1,i}sin\left(\omega_i t + \varphi_{1,i}\right) + E_{2,i}cos\left(\omega_i t + \varphi_{2,i}\right) \quad (9)$$

TABLE I
POWER STAGE PARAMETERS

Parameter	Symbol	Value
Power rating	P	2kVA
Nominal voltage amplitude	E_0	√2×110V
Nominal angular frequency	ω_0	2π60 rad.s^{-1}
Switching frequency	–	10 kHz
Inverter side inductance	$L_{1,i}$	1 mH
Line side inductance	$L_{2,i}$	0.2 mH
Filter capacitor	C_i	33 µF

where the voltage amplitude $E_{1,i}$ and $E_{2,i} \neq 0$, the frequency ω_i and phases $\varphi_{1,i}$ and $\varphi_{1,i}$, are unknowns. This signal can be modeled as follows,

$$\begin{cases} \dot{x}_1 = x_2 \\ \dot{x}_2 = -{\omega_i}^2 x_1 \\ y = \dfrac{k_1}{\lambda}x_1 + \dfrac{k_2}{\lambda}x_2 \end{cases} \quad (10)$$

The estimation of both signal state $(x_1, x_2)^T$ and frequency ω_i is intended. The following estimator is constructed considering $(x_1, x_2, x_3)^T$ as the estimator states while $e = (e_1, e_2, e_2)^T$ is the estimation error signals being $e_1 = x_1 - \hat{x}_1$, $e_2 = x_2 - \lambda\hat{x}_2$ and $e_3 = \hat{x}_3 - {\omega_i}^2$.

$$\begin{cases} \dot{\hat{x}}_1 = \lambda\hat{x}_2 + \dfrac{\lambda}{k_2}(y - \hat{y}) \\ \dot{\hat{x}}_2 = -\dfrac{\hat{x}_1\hat{x}_3}{\lambda} + \zeta(y - \hat{y}) \\ \dot{\hat{x}}_3 = -\gamma\hat{x}_1(y - \hat{y}) \\ \hat{y} = \dfrac{k_1}{\lambda}\hat{x}_1 + k_2\hat{x}_2 \end{cases} \quad (11)$$

The choice of arbitrary positive λ, ζ and γ, and nonzero k_1, k_2 coefficients ensures the convergence of the estimation error [32].

V. EVALUATION OF DAMPING PERFORMANCES

In this section, the efficacy of the proposed damping method is evaluated for a typical islanded MG composed of two identical DG units and one disturbing load.

C. Single DG unit

The efficacy of the proposed active damping method is firstly assessed for a single DG unit. For this aim, the expression (8) is simplified considering the linearized transfer function of the proposed disturbance observer.

$$v_{inv,i}^{*} = v_{inv,i} - D(s)v_{DG,i} \quad (12)$$

where, $D(s) = 1 - D'(s)$, being that $D'(s)$ is the linearized transfer function of the nonlinear estimator given by (11).

Accordingly, the DG system dynamic is reshaped by replacing the proposed resonance damping method given by (12) in (2), being that $v_{DG,i} = v_{PCC} + Z_{L_{2,i}}i_{DG,i}$.

$$v_{PCC} = \frac{G_{DG,i}}{1 + G_{DG,i}D(s)}v_{inv,i} - \frac{Z_{DG,i} + G_{DG,i}D(s)Z_{L_{2,i}}}{1 + G_{DG,i}D(s)}i_{DG,i} \quad (13)$$

The above equation can be simplified as

$$v_{PCC} = G_{DG,i}^{d}v_{inv,i} - Z_{DG,i}^{d}i_{DG,i} \quad (14)$$

where, $G_{DG,i}^{d}$ and $Z_{DG,i}^{d}$ represent, respectively, the damped voltage gain and equivalent output impedance expressions.

The frequency response of these expressions are illustrated in Fig. 7. By examining the obtained bode diagram, it appears

This article has been accepted for publication in a future issue of this journal, but has not been fully edited. Content may change prior to final publication. Citation information: DOI 10.1109/TIE.2019.2898611, IEEE Transactions on Industrial Electronics

clearly that the proposed damping method shows meaningful improvement in terms of resonance suppression. Indeed, it is shown that the resonance peak introduced by the LC-L filter with around 150dB is reduced to less than 5 dB without compromising the filter harmonic attenuation performances. Similarly, the equivalent output impedance tends to have a resistive behavior around the resonance frequency limiting both current and voltage resonance oscillations.

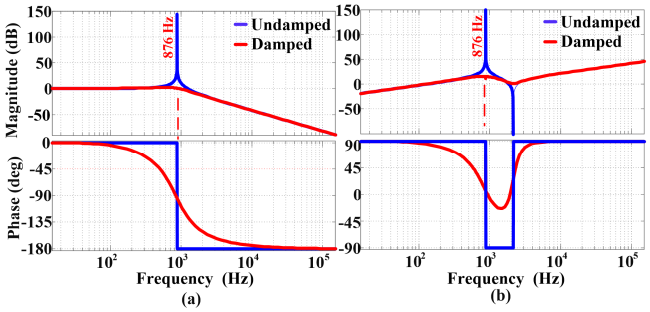

Fig. 7. Frequency response of the (a) voltage gain and (b) equivalent output impedance of DG #1 before and after damping

D. Multiple DG units

The effectiveness of the proposed damping method for resonance mitigation in islanded MGs is evaluated for a typical MG with two DG units ($N = 2$) and a single load ($M = 1$). Accordingly, the introduction of the proposed resonance damping method (12) in (5) results in the following expression:

$$v_{PCC} = G_1^d v_{inv,1} + G_2^d v_{inv,2} - Z_1^d i_{Load_{2,1}} \tag{15}$$

with,

$$G_1^d = \frac{G_{DG,1}^d Z_{DG,2}^d Z_{Load,1}}{Z_{DG,1}^d Z_{Load,1} + Z_{DG,2}^d Z_{Load,1} + Z_{DG,1}^d Z_{DG,2}^d}$$
$$G_2^d = \frac{G_{DG,2}^d Z_{DG,1}^d Z_{Load,1}}{Z_{DG,1}^d Z_{Load,1} + Z_{DG,2}^d Z_{Load,1} + Z_{DG,1}^d Z_{DG,2}^d} \tag{16}$$
$$Z_1^d = \frac{G_{Load,1}^d Z_{Load,1} Z_{DG,1}^d Z_{DG,2}^d}{Z_{DG,1}^d Z_{Load,1} + Z_{DG,2}^d Z_{Load,1} + Z_{DG,1}^d Z_{DG,2}^d}$$

where, G_1^d, G_2^d and Z_1^d represent the damped DG side voltage gains associated to DG#1 and DG#2, and the load side impedance expressions, respectively. $G_{DG,i}^d$ and $Z_{DG,i}^d$ are expressed in (14) and represent, respectively, the damped voltage gain and equivalent output impedance expressions associated to the i^{th} DG unit ($i = 1,2$). Considering identical DG units, the DGs side voltage gain expressions will be the same ($G_1^d = G_2^d$).

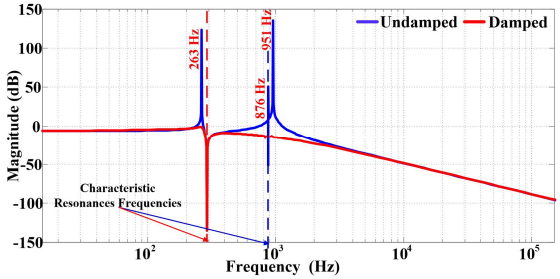

Fig. 8. Damped DG side voltage gain ($G_1^d = v_{pcc}/v_{inv,i}, i = 1,2$)

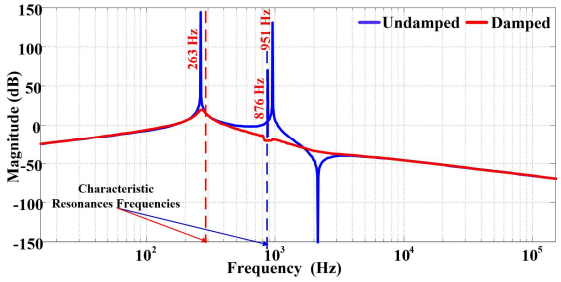

Fig. 9. Load side impedance ($Z_1^d = v_{pcc}/i_{Load_{2,1}}$)

The frequency response of these expressions, illustrated in Fig. 8-9, demonstrate the effectiveness of the proposed damping method that compensates effectively for resonances and limits their propagation in the islanded MG. Indeed, this method shows strong resonance mitigation performances addressing a challenging situation where a complex resonance characteristic prevails in the MG with resonances at various frequencies.

Moreover, the implementation of this method allows to reduce the resonance peak introduced by the load side circuit to a residual level that can be easily compensated by the inner control loops. This situation confirms that the proposed method extends the damping region enhancing MGs power quality and stability.

E. Stability analysis

The stabilizing effect of the proposed active damping method over the closed loop system is investigated based on the Nyquist plot representation of the open-loop transfer function. As shown in Fig.6, the control of each DG unit adopts a hierarchical structure wherein the first control stages include a cascaded voltage and current controller and a droop based power-sharing controller with a virtual output impedance. The voltage and current control expressions are given as follows:

$$G_{c,i}(s) = k_{pc,i} + k_c \sum_{h=1,odd}^{7} \frac{s}{s^2 + (\omega_0 h)^2} \tag{17}$$

$$G_{v,i}(s) = k_{pv,i} + k_v \sum_{h=1,odd}^{7} \frac{s}{s^2 + (\omega_0 h)^2} \tag{18}$$

where, $k_{pc,i}$ and $k_{pv,i}$, k_c and k_v represent, respectively, the proportional and resonant gains of the inner and outer loop controllers related the i[th] DG unit. ω_0 is the angular frequency.

Assuming a predominant inductive output impedance, the following droop based controller is adopted for power sharing, where the reactive power Q_i is controlled through the control of the filter-capacitor voltage amplitude, while the frequency is used to control the active power P_i.

$$\omega_{0,i} = \omega_0 - m_i \mathrm{P}_i - m_{d,i} \frac{d\mathrm{P}_i}{dt} \tag{19}$$

$$E_i = E_0 - n_i \mathrm{Q}_i - n_{d,i} \frac{d\mathrm{Q}_i}{dt} \tag{20}$$

where, n_i and m_i represent the proportional droop coefficients while $m_{d,i}$ and $n_{d,i}$ denote the derivative droop coefficients. E_i and $\omega_{0,i}$ denote the droped amplitude and

This article has been accepted for publication in a future issue of this journal, but has not been fully edited. Content may change prior to final publication. Citation information: DOI 10.1109/TIE.2019.2898611, IEEE Transactions on Industrial Electronics

frequency of the i[th] DG unit output voltage. After that, the virtual output impedance is integrated to enhance the inductive behavior of the output impedance and the following voltage reference is obtained

$$v^*_{DG,i} = E_i \sin\left(\omega_{0,i}\, t\right) - Z_{D,i} i_{DG,i} \quad (21)$$

where, $Z_{D,i} = L_{D,i} s$, represents the introduced i[th] DG virtual impedance, being $L_{D,i}$ the virtual inductance.

The dynamic of both voltage and current control loops is introduced considering the control parameters summarized in Table II. The closed loop dynamic of each DG unit can be derived by replacing the following control law in (2).

$$v_{inv,i} = \left(\left(v^*_{DG,i} - v_{DG,i}\right) C_v(s) - i_{inv,i}\right) C_c(s) \quad (22)$$

Being, $i_{inv,i} = i_{DG,i} + v_{DG,i}/Z_{c,i}$ the filter inductor current, and the filter capacitor voltage $v_{DG,i} = Z_{L_{2,i}} i_{DG,i} + v_{PCC}$.

Note that the dynamic of the adopted droop based power-sharing controller has been neglected in this part since it is much slower than the inner control loops while the virtual output inductance of $500\,\mu H$ has been lumped together with the load side filter inductance for the sake of simplicity. The resonant gains are set to zero since their effect is far from the frequency of concern and do not affect the stability analysis.

Accordingly, the closed loop dynamic of the i^{th} DG unit is obtained as follows:

$$v_{PCC} = \frac{G_{DG,i} C_{c,i} C_{v,i}}{1 + G_{DG,i}\, C_{c,i}\left(C_{v,i} Z_{c,i} + 1\right)/Z_{c,i}} v^*_{DG,i} - \frac{Z_{DG,i} + G_{DG,i} C_{c,i}\left(\left(C_{v,i} Z_{c,i} + 1\right) Z_{L_{2,i}} + Z_{c,i}\right)/Z_{c,i}}{1 + G_{DG,i}\, C_{c,i}\left(C_{v,i} Z_{c,i} + 1\right)/Z_{c,i}} i_{DG,i} \quad (23)$$

The above equation can be simplified as:

$$v_{PCC} = G_{CP,i} v^*_{DG,i} - Z_{CP,i} i_{DG,i} \quad (24)$$

where, $G_{CP,i}$ and $Z_{CP,i}$ represent the closed loop voltage gain and the equivalent output impedance, respectively.

The introduction of the proposed resonance damping method results in the following expression:

$$v_{PCC} = \frac{G^d_{DG,i} C_{c,i} C_{v,i}}{1 + G^d_{DG,i}\, C_{c,i}\left(C_{v,i} Z_{c,i} + 1\right)/Z_{c,i}} v^*_{DG,i} - \frac{Z^d_{DG,i} + G_{DG,i} C_{c,i}\left(\left(C_{v,i} Z_{c,i} + 1\right) Z_{L_{2,i}} + Z_{c,i}\right)/Z_{c,i}}{1 + G^d_{DG,i}\, C_{c,i}\left(C_{v,i} Z_{c,i} + 1\right)/Z_{c,i}} i_{DG,i} \quad (25)$$

The above equation can be simplified as

$$v_{PCC} = G^d_{CP,i} v^*_{DG,i} - Z^d_{CP,i} i_{DG,i} \quad (26)$$

Being, $G^d_{CP,i}$ and $Z^d_{CP,i}$, the damped closed loop voltage gain and equivalent output impedances expressions.

Fig. 10 illustrates the Nyquist plot around the critical point (−1, j0) for a single DG unit, with and without the proposed damping. In light of this result, the stabilisation effect of the proposed damping method is confirmed with sufficient phase and gain margins. Indeed, in contrast to the undamped system whose curves spiral to the infinity at the resonance frequency, the closed loop dynamic of the damped system is asymptotically stable since no open loop poles are found at the right hand plant and no encirclements of the point (−1, j0) are observed.

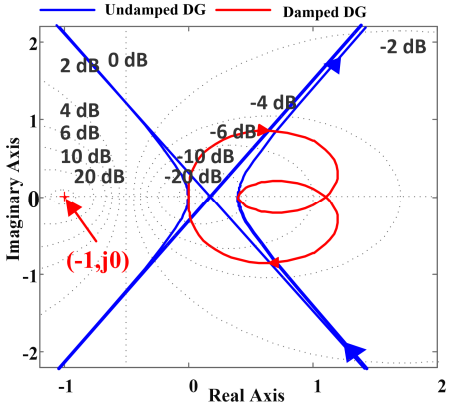

Fig. 10. Nyquist plots with and without active damping

F. Load power stability limit

The load impact on the system stability is investigated based on the Middlebrook impedance based stability analysis approach [36]. This approach investigates the interactions that occur in source-load circuits based on their representative impedances, namely, the equivalent output impedance of the closed loop controlled DG system, and the load input impedance, respectively given by $Z_{CP,i}$. $Z_{Load,j}$. According to this approach, the system stability is guaranteed as long as the inequality $|Z_{CP,i}| < |Z_{Load,j}|$ is verified. In other terms, the output impedance of the system should be maintained lesser than the load input impedance for the whole frequency range to avoid source-load interactions. Otherwise, when the system output impedance becomes higher than the load input impedance, the system stability is compromised and large resonance oscillations appears around the intersection frequencies of $|Z_{CP,i}|$and $|Z_{Load,j}|$. One solution, is either to sufficiently reduce the system output impedance magnitude or to increase the input load impedance at the intersection frequencies. However, and as reported in [37], this will reduce the maximum loadability of the system since the load input impedance is inversely proportional to the load power. Indeed, the load input impedance behave as a negative resistance of $-{V_{pcc}}^2/P_{Load}$ within the load bandwidth where V_{pcc} is the PCC voltage and P_{Load} is the load power.

In this way, and as illustrated in Fig.11, where the frequency response of $Z_{CP,i}$ and $Z_{Load,j}$ is illustrated for different load power conditions with and without damping, it appears that the load power limit stability of the undamped system is no larger than 10% of the full load condition. This is mainly due to the system output impedance that presents a high amplitude at the vicinity of the resonance frequency, which makes the system prone to source-load interactions and decreases its maximum loadability. Indeed, the stability of the undamped system get more worsened as the load power increases, so as the load input impedance decreases, since the interaction zone is widened and resonance oscillations are likely to appear at a lower frequency range affecting the whole system performances and stability. Besides, the introduction of the proposed damping method improves the system stability and extends the maximum loadability of the system since it

This article has been accepted for publication in a future issue of this journal, but has not been fully edited. Content may change prior to final publication. Citation information: DOI 10.1109/TIE.2019.2898611, IEEE Transactions on Industrial Electronics

reshapes the system output impedance and dampen out the resonance peak limiting the interaction with the load input impedance to higher load power ranges. In this sense, the system output impedance is separated from the input load impedance, which ensures initially the system stability for full load condition and extends its maximum loadability.

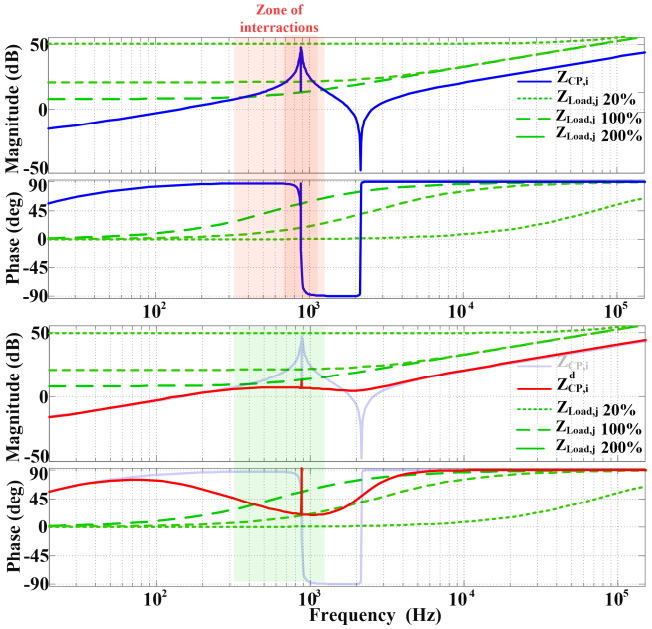

Fig. 11. Frequency response of the DG and load impedances (a) before damping with unstable characteristic and (b) after damping with stable characteristic.

G. Robustness analysis

The robustness stability of the proposed damping method is investigated based on the analysis of the system sensitivity to large system and load parameters variations including the variation of the inverter side filter inductance, filter capacitance and load side filter inductance with ± 80% from their nominal. These variations result in a challenging resonance picture with varying resonance frequencies. The system robustness is analyzed when the closed loop controlled DG unit is connected to a disturbing load. The dynamic of the system is obtained based on (24) and (4) as follows:

$$v_{PCC} = \frac{G_{CP,i}}{1 + Z_{CP,i}Y_{Load,j}} v^*_{DG,i} - \frac{Z_{CP,i}G_{Load,j}}{1 + Z_{CP,i}Y_{Load,j}} i_{Load_{2,j}} \quad (27)$$

In this case, the system stability no longer depends on the closed loop controlled DG unit, but also on the load dynamic. In this way, the system robustness to load input impedance variation is also analyzed. A common design specification in control theory states that the maximum value of the sensitivity transfer function, given by $S(s) = \left[1 + Z_{CP,i}Y_{Load,j}\right]^{-1}$, is closely related to the achievable stability margins. In this sense, for a given $M = \|S(s)\|_\infty$, the achievable stability margins would be greater than $M/(M-1)$ and $1/M$ [rad/s] for gain and phase margins, respectively [38]. More specifically, the sensitivity function should be lower than 6 dB to guarantee adequate stability margins with a gain margin of at least 6 dB and a phase margin of 29 while larger sensitivity values will result in weak performances and give rise to instability. In this way, and as illustrated in Fig.12 and Fig.13, the robustness of the proposed active damping method is verified for large system and load parameters variations since the corresponding sensitivity function, namely $S^d(s) = \left[1 + Z^d_{CP,i}Y_{Load,j}\right]^{-1}$, fits with the aforementioned stability requirements maintaining small values within a wide frequency range. It is shown that the introduction of the proposed damper improves for a large extent the system stability and provides an effective damping regardless to system and load parameters variations and accordingly regardless to resonances frequencies variation. This salient feature is particularly important in islanded as well as in grid-connected mode of microgrids operation wherein the grid impedance may vary within a wide range, which results similarly in challenging resonance characteristics. Moreover, the proposed damping method presents advantageous performances even when the resonance frequencies vary within a wide frequency range and resonances move across the critical frequency.

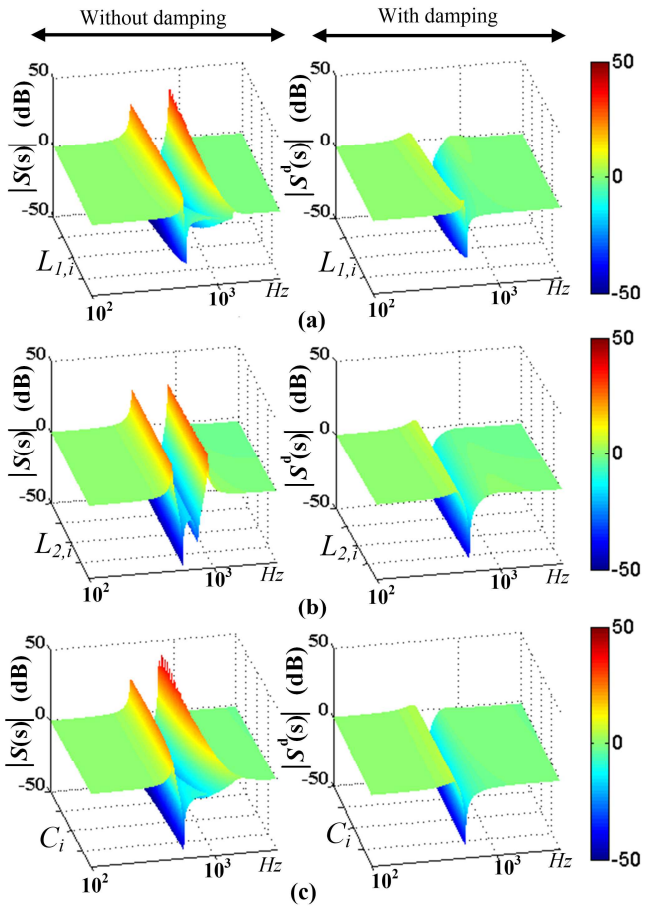

Fig. 12. System sensitivity to system parameters variation. (a) $L_{1,i}$: 1 mH ± 80%. (b) $L_{2,i}$: 200 μH ± 80%. (c) C_i 33 μF ± 80%.

This article has been accepted for publication in a future issue of this journal, but has not been fully edited. Content may change prior to final publication. Citation information: DOI 10.1109/TIE.2019.2898611, IEEE Transactions on Industrial Electronics

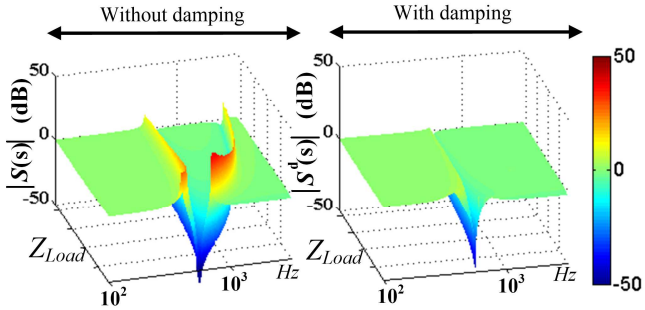

Fig. 13. System sensitivity to load impedance variation with $Z_{load,\,j}$ ± 80%.

VI. EXPERIMENTAL VALIDATION

As shown in Fig. 14, a MG based on two DGs was built in order to evaluate the proposed control strategy and verify its efficacy for resonance damping. The experimental test bench comprises two SEMIKRON inverters with constant DC power sources and similar LC-L output filters supplying either a linear or a rectifier type nonlinear filter interfaced loads.

The overall control strategy, shown in Fig. 6, including the proposed resonance damping method and both voltage and power sharing control levels is implemented on a dSPACE Micro Auto Box control prototyping system based on the parameters listed in Table II. The execution time is of 44.6 µs whose only 6.1 µs are necessary to implement the proposed resonance damping method.

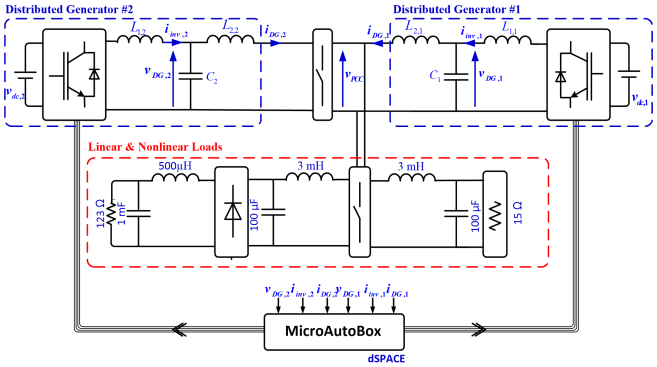

Fig. 14. Configuration of the islanded MG

TABLE II
CONTROL PARAMETERS

Parameter	Symbol	Value
Current controller gains	k_{pc}	5.21
	k_c	60
Voltage controller gains	k_{pv}	2.58
	k_v	70
Frequency droop coefficients	m_i	0.003 rad.s^{-1}.W^{-1}
	$m_{d,i}$	0.00004 rad.W^{-1}
Amplitude droop coefficients	n_i	0.005 V.Var^{-1}
	$n_{d,i}$	0.00003 V.s. Var^{-1}
Damping coefficient	k_d	1
Estimator parameters	λ, ζ, γ	100, 200, 500
	k_1, k_2	0.01, 0.001

Several tests are performed to evaluate the efficacy of the proposed damping method in terms of resonance mitigation and stability enhancement. Indeed, this system is initially stable, but presents a lack of resonance damping and remains prone to resonance instabilities. As shown in Fig.4 and 5, the analysis of this system based on (7) reveals the presence of resonances at the vicinity of 263 Hz, 876 Hz and 951 Hz, with a magnitude of 144 dB, 50 dB and 141 dB, respectively. The control gains are adjusted to control the resonance excitation until a resonating or even destabilized dynamic is obtained. Indeed, the proportional gains of the inner current control loops corresponding to each DG unit are gradually increased in such a way to reduce their corresponding phase margins and raise mutual resonance interactions. The measured voltage and current waveforms including the filter capacitor voltage of each DG unit, the load bus voltage measured at the PCC, the damping signal and the corresponding line currents are reported through Fig.15 to 20 before and after the proposed damping method is enabled for two main cases.

The first test case evaluates the performance of the proposed damping method against small resonance perturbations. The analysis of the measured voltage and current waveforms shown in Fig 15 and 16 shows the presence of low order harmonic components due to resonance excitation. Indeed, it is clear that at least one resonance is excited given that low order resonance harmonics rise around 970 Hz similarly in both voltage and current waveforms and propagates in the whole MG, which is consistent with the above analysis. Meanwhile, it is shown that the introduction of the proposed damping method provides sufficient damping performances to dampen out the resulting resonance harmonics and limit their propagation in the whole MG. Note that, the amplitude of the damping signal does not exceed 10% of the voltage control signal. Moreover, the MG preserves suitable performances for both voltage tracking and power sharing, which confirms that the introduction of the damping control signal does not engage the performances of the inners control loops. This situation improves significantly the power quality and stability of the islanded MG.

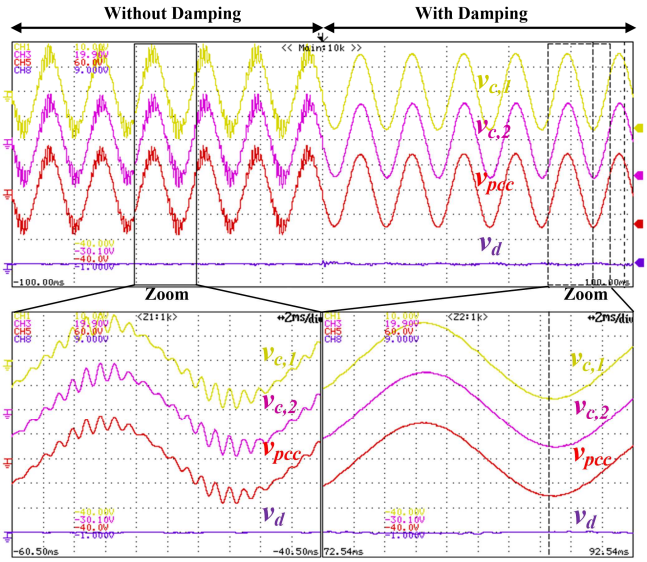

Fig.15. Experimental test results for an islanded MG: Voltage waveforms measured at the PCC, DG #1 and DG #2, and the damping signal (×10) before and after damping [top: (x-axis: 100ms/div; y-axis: 100V/div)] and enlarged waveforms [bottom: (x-axis: 2ms/div)]

This article has been accepted for publication in a future issue of this journal, but has not been fully edited. Content may change prior to final publication. Citation information: DOI 10.1109/TIE.2019.2898611, IEEE Transactions on Industrial Electronics

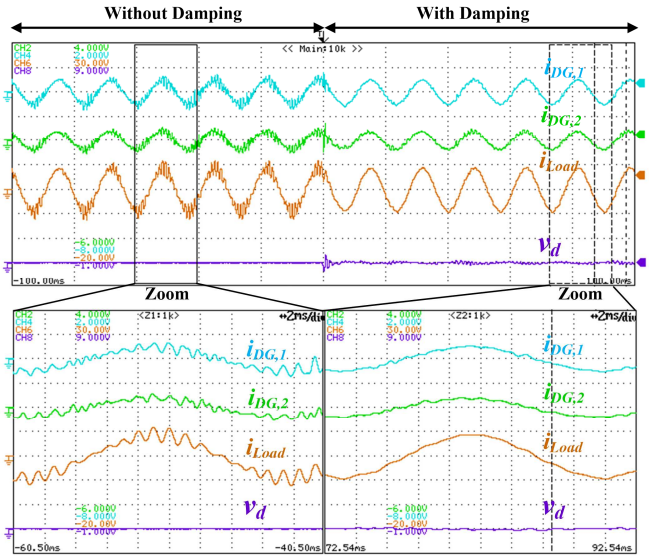

Fig.16. Experimental test results for an islanded MG: Measured Load, DG #1 and DG #2 line current waveforms for a disturbing linear load before and after applying the damper [top: (x-axis: 100ms/div; y-axis: 10A/div)] and enlarged waveforms [bottom: (x-axis: 2ms/div; y-axis: 10A/div)].

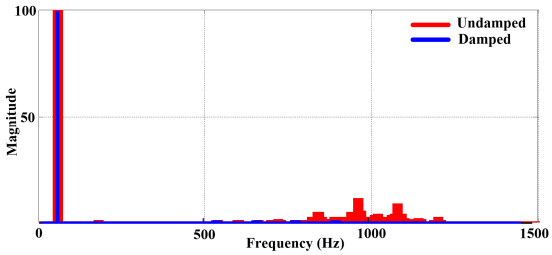

Fig.17. Voltage harmonic spectrum before and after damping – case #1

The second test case evaluates the stabilizing performances of the proposed damping method when resonance interactions become more severe and turn the whole system to be unstable. The obtained test results are reported in Fig. 18 and 19 illustrating both voltage and current waveforms with and without damping. The measured voltage and current waveforms show initially an unstable dynamic with very high resonance oscillations propagating to the whole MG. Indeed, the associated harmonic spectra shown in Fig. 20 confirms similarly for both voltage and current waveforms the presence of very high resonance components. In addition, it depicts that resonances are excited around 970 Hz, with noticeable amplification at 850 Hz and 1090 Hz, which is consistent with the analysis developed in Section III, and confirms the validity of the proposed MG modeling for resonance investigation. In this case, resonance oscillations with very high magnitudes, well above 100% of the associated fundamental component, are noticed until the proposed resonance damping method is enabled.

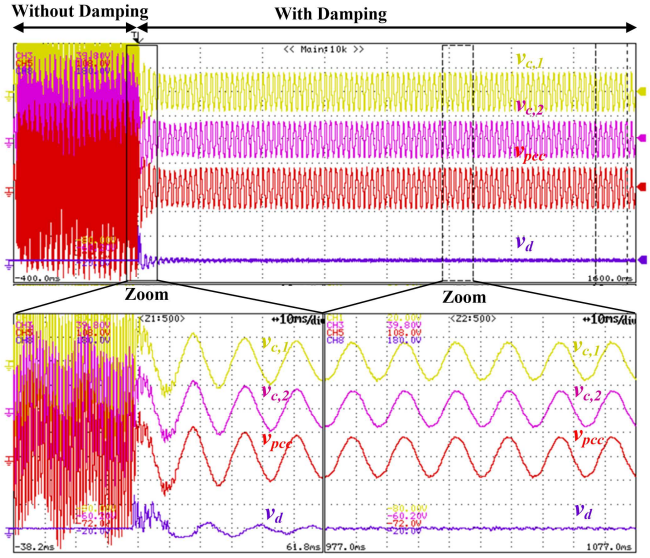

Fig.18. Experimental test results for an islanded MG: Voltage waveforms measured at the PCC, DG #1 and DG #2, and the damping signal (×10) for an unstable case before and after damping [top: (x-axis: 1.6s/div; y-axis: 180V/div)] and enlarged waveforms [bottom: (x-axis: 10ms/div)]

It is clearly shown that the introduction of the proposed resonance damping method is highly effective to dampen out the unstable dynamic of islanded MGs limiting both resonance harmonic amplification and propagation. The proposed method was able to properly mitigate both transient and steady-state resonance guaranteeing the large signal stability of the islanded MG within few periods.

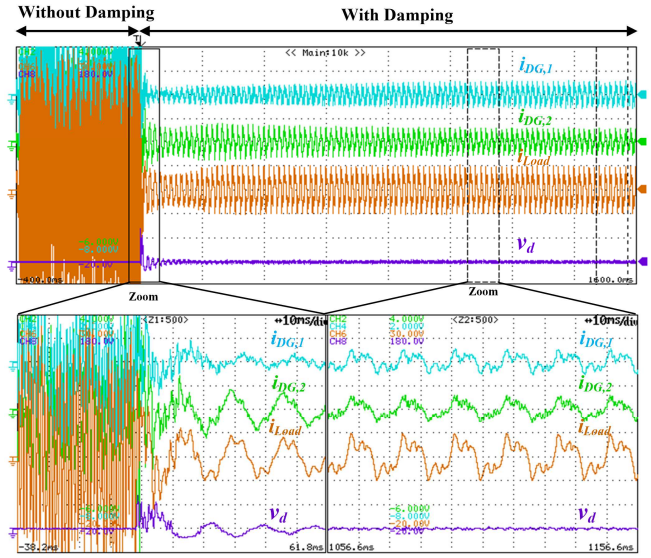

Fig.19. Experimental test results for an islanded MG: Measured Load, DG #1 and DG #2 line current waveforms for an unstable case before and after applying the damper [top: (x-axis: 1.6s/div; y-axis: 10A/div)] and enlarged waveforms [bottom: (x-axis: 10ms/div; y-axis: 10A/div)].

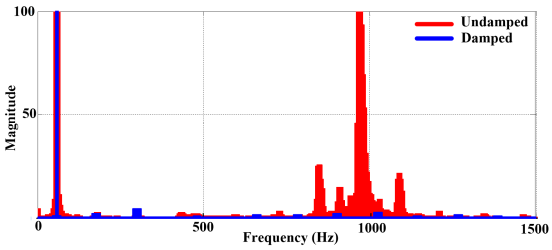

Fig.20. voltage harmonic spectrum before and after damping – case #2

VII. Conclusion

In this paper, the resonances characteristics of islanded MGs with multiple MGs and loads has been analyzed using simplified passive circuit representations. After that, an effective damping method was proposed to address resonances issues encountered in DG based MGs based on a robust disturbance observer. From a practical point of view, the design of the proposed damping method does not depends on the prior knowledge of system parameters, which is particularly important in scalable MGs. Moreover, the implementation of this method does not affect neither the dynamic performances of DGs controllers nor the harmonic attenuation capability of the filtering stages. The effectiveness of the proposed resonance damping method has been verified using simulations and experiments. It was shown, that the proposed method is highly effective to dampen out the unstable dynamic of islanded MGs limiting both resonance harmonic amplification and propagation.

References

[1] X. Liang, "Emerging Power Quality Challenges Due to Integration of Renewable Energy Sources," *IEEE Trans. Ind. Appl.*, vol. 53, no. 2, pp. 855–866, Mar. 2017.

[2] S. Kumar Tiwari, B. Singh, and P. K. Goel, "Design and Control of Microgrid Fed by Renewable Energy Generating Sources," *IEEE Trans. Ind. Appl.*, vol. 54, no. 3, pp. 2041–2050, May 2018.

[3] G. G. Talapur, H. Suryawanshi, L. Xu, and A. Shitole, "A Reliable Micro-grid with Seamless Transition between Grid Connected and Islanded Mode for Residential Community with Enhanced Power Quality," *IEEE Trans. Ind. Appl.*, pp. 1–1, 2018.

[4] W. R. Issa, A. H. El Khateb, M. A. Abusara, and T. K. Mallick, "Control Strategy for Uninterrupted Microgrid Mode Transfer During Unintentional Islanding Scenarios," *IEEE Trans. Ind. Electron.*, vol. 65, no. 6, pp. 4831–4839, Jun. 2018.

[5] J. M. Guerrero, J. C. Vasquez, J. Matas, L. G. de Vicuna, and M. Castilla, "Hierarchical Control of Droop-Controlled AC and DC Microgrids—A General Approach Toward Standardization," *IEEE Trans. Ind. Electron.*, vol. 58, no. 1, pp. 158–172, Jan. 2011.

[6] Z. Li, C. Zang, P. Zeng, H. Yu, and S. Li, "Fully Distributed Hierarchical Control of Parallel Grid-Supporting Inverters in Islanded AC Microgrids," *IEEE Trans. Ind. Informatics*, vol. 14, no. 2, pp. 679–690, Feb. 2018.

[7] B. Liu, Q. Wei, C. Zou, and S. Duan, "Stability Analysis of LCL-Type Grid-Connected Inverter Under Single-Loop Inverter-Side Current Control With Capacitor Voltage Feedforward," *IEEE Trans. Ind. Informatics*, vol. 14, no. 2, pp. 691–702, Feb. 2018.

[8] M. Lu, X. Wang, P. C. Loh, and F. Blaabjerg, "Resonance Interaction of Multiparallel Grid-Connected Inverters With LCL Filter," *IEEE Trans. Power Electron.*, vol. 32, no. 2, pp. 894–899, Feb. 2017.

[9] Xiongfei Wang, F. Blaabjerg, and Zhe Chen, "Autonomous Control of Inverter-Interfaced Distributed Generation Units for Harmonic Current Filtering and Resonance Damping in an Islanded Microgrid," *IEEE Trans. Ind. Appl.*, vol. 50, no. 1, pp. 452–461, Jan. 2014.

[10] S. Jayalath and M. Hanif, "Generalized LCL-Filter Design Algorithm for Grid-Connected Voltage-Source Inverter," *IEEE Trans. Ind. Electron.*, vol. 64, no. 3, pp. 1905–1915, Mar. 2017.

[11] J. Chen and J. Chen, "Stability Analysis and Parameters Optimization of Islanded Microgrid With Both Ideal and Dynamic Constant Power Loads," *IEEE Trans. Ind. Electron.*, vol. 65, no. 4, pp. 3263–3274, Apr. 2018.

[12] Y. Han, P. Shen, X. Zhao, and J. M. Guerrero, "Control Strategies for Islanded Microgrid Using Enhanced Hierarchical Control Structure With Multiple Current-Loop Damping Schemes," *IEEE Trans. Smart Grid*, vol. 8, no. 3, pp. 1139–1153, May 2017.

[13] Y. Han, H. Li, P. Shen, E. A. A. Coelho, and J. M. Guerrero, "Review of Active and Reactive Power Sharing Strategies in Hierarchical Controlled Microgrids," *IEEE Trans. Power Electron.*, vol. 32, no. 3, pp. 2427–2451, Mar. 2017.

[14] Y. Sun, X. Hou, J. Yang, H. Han, M. Su, and J. M. Guerrero, "New Perspectives on Droop Control in AC Microgrid," *IEEE Trans. Ind. Electron.*, vol. 64, no. 7, pp. 5741–5745, Jul. 2017.

[15] A. Micallef, M. Apap, C. Spiteri-Staines, and J. M. Guerrero, "Mitigation of Harmonics in Grid-Connected and Islanded Microgrids Via Virtual Admittances and Impedances," *IEEE Trans. Smart Grid*, pp. 1–11, 2015.

[16] W. Wu, Y. Liu, Y. He, H. S.-H. Chung, M. Liserre, and F. Blaabjerg, "Damping Methods for Resonances Caused by LCL-Filter-Based Current-Controlled Grid-Tied Power Inverters: An Overview," *IEEE Trans. Ind. Electron.*, vol. 64, no. 9, pp. 7402–7413, Sep. 2017.

[17] W. Wu, Y. He, T. Tang, and F. Blaabjerg, "A New Design Method for the Passive Damped LCL and LLCL Filter-Based Single-Phase Grid-Tied Inverter," *IEEE Trans. Ind. Electron.*, vol. 60, no. 10, pp. 4339–4350, Oct. 2013.

[18] C. C. Gomes, A. F. Cupertino, and H. A. Pereira, "Damping techniques for grid-connected voltage source converters based on LCL filter: An overview," *Renew. Sustain. Energy Rev.*, vol. 81, pp. 116–135, Jan. 2018.

[19] X. Li, X. Wu, Y. Geng, X. Yuan, C. Xia, and X. Zhang, "Wide Damping Region for LCL-Type Grid-Connected Inverter With an Improved Capacitor-Current-Feedback Method," *IEEE Trans. Power Electron.*, vol. 30, no. 9, pp. 5247–5259, Sep. 2015.

[20] Y. Geng, Y. Yun, R. Chen, K. Wang, H. Bai, and X. Wu, "Parameters Design and Optimization for LC-Type Off-Grid Inverters With Inductor-Current Feedback Active Damping," *IEEE Trans. Power Electron.*, vol. 33, no. 1, pp. 703–715, Jan. 2018.

[21] Z. Xin, P. C. Loh, X. Wang, F. Blaabjerg, and Y. Tang, "Highly Accurate Derivatives for LCL-Filtered Grid Converter With Capacitor Voltage Active Damping," *IEEE Trans. Power Electron.*, vol. 31, no. 5, pp. 3612–3625, May 2016.

[22] W. Yao, Y. Yang, X. Zhang, F. Blaabjerg, and P. C. Loh, "Design and Analysis of Robust Active Damping for LCL Filters Using Digital Notch Filters," *IEEE Trans. Power Electron.*, vol. 32, no. 3, pp. 2360–2375, Mar. 2017.

[23] R. Pena-Alzola, M. Liserre, F. Blaabjerg, R. Sebastian, J. Dannehl, and F. W. Fuchs, "Systematic Design of the Lead-Lag Network Method for Active Damping in LCL-Filter Based Three Phase Converters," *IEEE Trans. Ind. Informatics*, vol. 10, no. 1, pp. 43–52, Feb. 2014.

[24] D. J. L. M. F. F, "Filter-Based Active Damping of Voltage Source Converters With LCL Filter," *IEEE Trans. Ind. Electron.*, vol. 58, no. 8, pp. 3623–3633, 2011.

[25] Q. Qian, S. Xie, L. Huang, J. Xu, Z. Zhang, and B. Zhang, "Harmonic Suppression and Stability Enhancement for Parallel Multiple Grid-Connected Inverters Based on Passive Inverter Output Impedance," *IEEE Trans. Ind. Electron.*, vol. 64, no. 9, pp. 7587–7598, Sep. 2017.

[26] R. Pena-Alzola, M. Liserre, F. Blaabjerg, M. Ordonez, and T. Kerekes, "A Self-commissioning Notch Filter for Active Damping in a Three-Phase LCL -Filter-Based Grid-Tie Converter," *IEEE Trans. Power Electron.*, vol. 29, no. 12, pp. 6754–6761, Dec. 2014.

[27] D. Yang, X. Ruan, and H. Wu, "Impedance Shaping of the Grid-Connected Inverter with LCL Filter to Improve Its Adaptability to the Weak Grid Condition," *IEEE Trans. Power Electron.*, vol. 29, no. 11, pp. 5795–5805, Nov. 2014.

[28] J. He, Y. W. Li, D. Bosnjak, and B. Harris, "Investigation and Active Damping of Multiple Resonances in a Parallel-Inverter-Based Microgrid," *IEEE Trans. Power Electron.*, vol. 28, no. 1, pp. 234–246, Jan. 2013.

[29] J. He, Y. W. Li, R. Wang, and C. Zhang, "Analysis and Mitigation of Resonance Propagation in Grid-Connected and Islanding Microgrids,"

IEEE Trans. Energy Convers., vol. 30, no. 1, pp. 70–81, Mar. 2015.
[30] W.-H. Chen, J. Yang, L. Guo, and S. Li, "Disturbance-Observer-Based Control and Related Methods—An Overview," *IEEE Trans. Ind. Electron.*, vol. 63, no. 2, pp. 1083–1095, Feb. 2016.
[31] G. Obregon-Pulido, B. Castillo-Toledo, and A. Loukianov, "A globally convergent estimator for n-frequencies," *IEEE Trans. Automat. Contr.*, vol. 47, no. 5, pp. 857–863, May 2002.
[32] E. Hossain, R. Perez, A. Nasiri, and R. Bayindir, "Stability improvement of microgrids in the presence of constant power loads," *Int. J. Electr. Power Energy Syst.*, vol. 96, pp. 442–456, Mar. 2018.
[33] B. Chen, G. Pin, W. M. Ng, C. K. Lee, S. Y. R. Hui, and T. Parisini, "An Adaptive Observer-Based Switched Methodology for the Identification of a Perturbed Sinusoidal Signal: Theory and Experiments," *IEEE Trans. Signal Process.*, vol. 62, no. 24, pp. 6355–6365, Dec. 2014.
[34] B. Chen, G. Pin, W. M. Ng, S. Y. R. Hui, and T. Parisini, "An Adaptive-Observer-Based Robust Estimator of Multi-sinusoidal Signals," *IEEE Trans. Automat. Contr.*, vol. 63, no. 6, pp. 1618–1631, Jun. 2018.
[35] B. Chen, G. Pin, W. M. Ng, P. Li, T. Parisini, and S.-Y. R. Hui, "Online Detection of Fundamental and Interharmonics in AC Mains for Parallel Operation of Multiple Grid-Connected Power Converters," *IEEE Trans. Power Electron.*, pp. 1–1, 2018.
[36] R. D. MIDDLEBROOK and S. ĆUK, "A general unified approach to modelling switching-converter power stages," *Int. J. Electron.*, vol. 42, no. 6, pp. 521–550, Jun. 1977.
[37] X. Zhang, X. Ruan, and Q.-C. Zhong, "Improving the Stability of Cascaded DC/DC Converter Systems via Shaping the Input Impedance of the Load Converter With a Parallel or Series Virtual Impedance," *IEEE Trans. Ind. Electron.*, vol. 62, no. 12, pp. 7499–7512, Dec. 2015.
[38] S. Skogestad and I. Postlethwaite, *Multivariable feedback control : analysis and design*. John Wiley, 2005.

Abdelhakim Saim was born in Batna, Algeria, on February 02, 1990. He received the B.S. and the M.S. degrees in electronics and control engineering both from Blida University, Algeria, in 2010 and 2012, respectively, and the Ph.D. degree in control engineering from Tizi-Ouzou University, Algeria, in 2017. Since 2017, he has been an Assistant Professor with the Department of Control and Instrumen-tation, University of Sciences and Technology Houari Boumediene, Algiers, Algeria. His current research deals with the power quality and stability of microgrids.

Azeddine Houari received the Engineer degree in 2008 from Bejaia University, Algeria, and a Ph.D. degree in 2012 from Lorraine University, France. Since 2014, he works as an Assistant Professor at Nantes University, France, and exercises his research activities with the Institut de Recherche en Energie Electrique de Nantes Atlantique (IREENA). His current research deals with the power quality and the stability issues in stationary and embedded DC and AC micro-grids.

Josep M. Guerrero (S'01-M'04-SM'08-FM'15) received the B.S. degree in telecommunications engineering, the M.S. degree in electronics engineering, and the Ph.D. degree in power electronics from the Technical University of Catalonia, Barcelona, in 1997, 2000 and 2003, respectively. Since 2011, he has been a Full Professor with the Department of Energy Technology, Aalborg University, Denmark, where he is responsible for the Microgrid Research Program (www.microgrids.et.aau.dk). From 2014 he is chair Professor in Shandong University; from 2015 he is a distinguished guest Professor in Hunan University; and from 2016 he is a visiting professor fellow at Aston University, UK, and a guest Professor at the Nanjing University of Posts and Telecommunications.

His research interests is oriented to different microgrid aspects, including power electronics, distributed energy-storage systems, hierarchical and cooperative control, energy management systems, smart metering and the internet of things for AC/DC microgrid clusters and islanded minigrids; recently specially focused on maritime microgrids for electrical ships, vessels, ferries and seaports. Prof. Guerrero is an Associate Editor for a number of IEEE TRANSACTIONS. He has published more than 450 journal papers in the fields of microgrids and renewable energy systems, which are cited more than 30,000 times. He received the best paper award of the IEEE Transactions on Energy Conversion for the period 2014-2015, and the best paper prize of IEEE-PES in 2015. As well, he received the best paper award of the Journal of Power Electronics in 2016. During five consecutive years, from 2014 to 2018, he was awarded by Thomson Reuters as Highly Cited Researcher. In 2015 he was elevated as IEEE Fellow for his contributions on "distributed power systems and microgrids."

Ali Djerioui was born in M'Sila, Algeria, in 1986. In 2009, he received the Engineer degree in electrical engineering from the University of M'Sila, Algeria. He received M.Sc. degree in electrical engineering from the Polytechnic Military Academy and Ph.D. degree in electronic instrumentation systems from University of Sciences and Technology Houari Boumediene, Algiers, Algeria, in 2011 and 2016, respectively. He is currently an Associate Professor with the Department of Electronics, M'Sila University, Algeria. His current research interests include power electronics, control, microgrids and power quality.

Mohamed Machmoum was born in Casablanca, Morocco, on November 29, 1961. He received the Engineering Degree in 1984 from the "Institut Supérieur Industriel" of Liège, Belgium, the Master and Ph.D. degrees from the "Institut National Polytechnique of Lorraine (INPL)", France, respectively in 1985 and 1989, all in electrical engineering. In 1991, he joined "l'Ecole Polytechnique de l'Université de Nantes" as Assistant Professor. Since September 2005, he is a full Professor at the same Engineering School.

He is actually the head of IREENA laboratory, University of Nantes. His main area of interest includes power electronics, power quality, wind and tidal energy conversion systems and microgrids. He has supervised in these fields more than 25 Ph.D. and published one book related to modeling of electrical machines, several chapter books and nearly 240 journals and conferences in his area of expertise.

Mourad Ait Ahmed was born in Djelfa, Algeria, on June 21, 1965. In 1988 he received the Engineer degree in electrical engineering (Automatic Control option) from Ecole Nationale des Ingénieurs et des Techniciens d'Algérie (ENITA), Algeria. In 1993, he obtained his Ph.D. degree in Robotic at Université Paul Sabatier (LAAS-CNRS), Toulouse, France. He is now at the Departement of Electrical Engineering, Ecole Polytechnique de l'Université de Nantes, Saint-Nazaire, France, where he is an Associate Professor in automatic control. His main research interests are in the fields of modeling and control of electrical machines and networks, with as applications wind and tidal energy conversion, microgrids and embedded electrical network.